ISSN 1674-1056
http://cpb.iphy.ac.cn
http://iopscience.iop.org/cpb
中国物理 B
Chinese Physics
中国物理 Chinese Physics B

Effect of Hf^{4+} doping on structure and enhancement of upconversion luminescence in Yb: Tm: $LiNbO_3$crystals

Li Dai(代丽), Chunrui Liu(刘春蕊), Xianbo Han(韩县博), Luping Wang(王路平), Yu Shao(邵瑀), Yuheng Xu(徐玉恒)

Citation: Chin. Phys. B . 2018, 27(11): 114217. **doi:** 10.1088/1674-1056/27/114217
Journal homepage: http://cpb.iphy.ac.cn; http://iopscience.iop.org/cpb

What follows is a list of articles you may be interested in

Optical properties of a three-dimensional chiral metamaterial

Juan-Juan Guo(郭娟娟), Mao-Sheng Wang(汪茂胜), Wan-Xia Huang(黄万霞)

Chin. Phys. B . 2017, 26(12): 124211. **doi:** 10.1088/1674-1056/26/12/124211

Optical properties of Mg^{2+}, Yb^{3+}, and Ho^{3+} tri-doped $LiNbO_3$ crystals

Li Dai(代丽), Chun-Rui Liu(刘春蕊), Chao Tan(谭超), Zhe-Hua Yan(阎哲华), Yu-Heng Xu(徐玉恒)

Chin. Phys. B . 2017, 26(4): 044207. **doi:** 10.1088/1674-1056/26/4/044207

Photoluminescence characteristics of ZnTe bulk crystal and ZnTe epilayer grown on GaAs substrate by MOVPE

Lü Hai-Yan, Mu Qi, Zhang Lei, Lü Yuan-Jie, Ji Zi-Wu, Feng Zhi-Hong, Xu Xian-Gang, Guo Qi-Xin

Chin. Phys. B . 2015, 24(12): 124207. **doi:** 10.1088/1674-1056/24/12/124207

Design and optimization of a SiC thermal emitter/absorber composed of periodic microstructures based on a non-linear method

Wang Wei-Jie, Zhao Zhen-Guo, Zhao Yi, Zhou Hai-Jing, Fu Ce-Ji

Chin. Phys. B . 2015, 24(9): 094213. **doi:** 10.1088/1674-1056/24/9/094213

Influences of Mg^{2+} ion on dopant occupancy and upconversion luminescence of Ho^{3+} ion in $LiNbO_3$crystal

Dai Li, Xu Chao, Zhang Ying, Li Da-Yong, Xu Yu-Heng

Chin. Phys. B . 2013, 22(9): 094201. **doi:** 10.1088/1674-1056/22/9/094201

Effect of Hf^{4+} doping on structure and enhancement of upconversion luminescence in Yb:Tm:$LiNbO_3$ crystals*

Li Dai(代丽)[1,†], Chunrui Liu(刘春蕊)[1], Xianbo Han(韩县博)[1], Luping Wang(王路平)[2], Yu Shao(邵瑀)[1], and Yuheng Xu(徐玉恒)[3]

[1] College of Science, Harbin University of Science and Technology, Harbin 150080, China
[2] School of Materials Science and Engineering, Harbin University of Science and Technology, Harbin 150040, China
[3] Department of the Applied Chemistry, Harbin Institute of Technology, Harbin 150001, China

(Received 26 April 2018; revised manuscript received 3 July 2018; published online 19 October 2018)

A series of Yb:Tm:$LiNbO_3$ crystals doped with x mol% Hf^{4+} ions ($x = 2$, 4, and 6) were grown by the Czochralski method. The dopant occupancy and defect structure of Hf:Yb:Tm:$LiNbO_3$ crystals were investigated by x-ray diffraction and infrared transmission spectra. The influence of Hf^{4+} ions concentration on UV–VIS–NIR absorption spectra of Hf:Yb:Tm:$LiNbO_3$ crystals was discussed. The upconversion luminescence of Hf:Yb:Tm:$LiNbO_3$ crystals was obtained under 980 nm excitation. Strong emissions were observed at 475 nm in the blue wavelength range and 651 nm in the red wavelength range. Remarkably, enhancement of the red and blue upconversion luminescence was achieved by tridoping Hf^{4+} ions.

Keywords: Hf:Yb:Tm:$LiNbO_3$ crystals, crystal structure, upconversion luminescence

PACS: 42.70.–a, 61.50.Ah, 78.55.–m **DOI:** 10.1088/1674-1056/27/11/114217

1. Introduction

Recently, rare-earths (RE) ions doped optical materials with the characteristic of efficient upconversion luminescence from infrared (IR) to visible radiation[1,2] attract considerable attention due to their potential applications in solid-state lasers, optical communications, solar cell, biological fluorescence labels, and so on.[3,4] Upconversion emission is usually obtained in bulk materials with relatively low phonon energy,[5] which decreases multiphonon relaxation rate and increases the lifetimes of the intermediate metastable states.[6] $LiNbO_3$ crystals with low phonon energy are promising matrices for upconversion luminescence due to their good mechanical performance, high stability, excellent electro-optic, acousto-optic, nonlinear optic, and piezoelectric performances.[7–9] To obtain efficient upconversion luminescence, RE ions such as Er^{3+}, Tm^{3+}, Nd^{3+}, and Ho^{3+} doped $LiNbO_3$ crystals have been studied for many years. Among them, Tm^{3+} ion is well known as an activator of blue ($^1G_4 \rightarrow {}^3H_6$ transition), red ($^1G_4 \rightarrow {}^3F_4$ and $^3F_3 \rightarrow {}^3H_6$ transitions), and NIR ($^3H_4 \rightarrow {}^3H_6$ and $^3F_4 \rightarrow {}^3H_6$ transitions) emissions.[1,10,11] It is noteworthy that Tm^{3+} ions can be applied to blue laser which exhibits applications in optical communication, color display, and so on. Although upconversion luminescence of Tm^{3+} ions can be obtained under 980 nm excitation, the absorption of Tm^{3+} ions at the pumping wavelength is weak. While, as a sensitizer, Yb^{3+} ion can strongly absorb the pumping light and transfer energy to Tm^{3+} ions, which increases the pumping light absorption efficiency and lowers the laser threshold.[10,12] The upconversion luminescence of Yb^{3+} and Tm^{3+} codoped $LiNbO_3$ crystals has been reported by Xing *et al.*[13]

As we all know, the application of Yb:Tm:$LiNbO_3$ crystal in frequency doubler and laser medium material is limited by the photorefractive damage and the problem can be overcome by doping anti-photorefractive ions such as Mg^{2+}, Zn^{2+}, Sc^{3+}, In^{3+}, Hf^{4+}, and Zr^{4+} ions.[14–19] It is worthy of notice that luminescence behavior can be improved by doping anti-photorefractive ions.[20] Recently, a few reports have researched the influence of anti-photorefractive ions on upconversion emission in RE^{3+} ions doped $LiNbO_3$ crystals.[20–22] Shur *et al.* found that the addition of ZrO_2 enhanced the 470 nm emission of Tm:$LiNbO_3$ in blue wavelength region.[21] Sun *et al.* reported that 1.5 mol% In_2O_3 enhanced the 1.5 μm emission but suppressed 550 nm green upconversion emission of Er:$LiNbO_3$.[22] Hf^{4+} has been reported to be an effective ion to improve the anti-photorefractive property of $LiNbO_3$, while the effect of Hf^{4+} on the optical properties of Yb:Tm:$LiNbO_3$ crystals have not been reported.

In this paper, Hf:Yb:Tm:$LiNbO_3$ crystals with varying Hf^{4+} concentrations (2 mol%, 4 mol%, and 6 mol%) were successfully grown by the Czochralski technique. The defect structure was analyzed by x-ray diffraction (XRD) and infrared (IR) transmission spectra. The UV–VIS–NIR absorption spectra of Hf:Yb:Tm:$LiNbO_3$ crystals were discussed.

*Project supported by Special Funds of Harbin Innovation Talents in Science and Technology Research, China (Grant No. 2015RQQXJ045) and Science Funds for the Young Innovative Talents of HUST, China.

†Corresponding author. E-mail: daili198108@126.com

© 2018 Chinese Physical Society and IOP Publishing Ltd

The effect of Hf^{4+} ions on the upconversion luminescence of Hf:Yb:Tm:$LiNbO_3$ crystals was investigated under 980 nm excitation. A new strategy to improve the properties of red and blue upconversion luminescence of Yb:Tm:$LiNbO_3$ crystals is given in this paper.

2. Experimental details

2.1. Crystal growth

The congruent Hf:Yb:Tm:$LiNbO_3$ crystals ([Li]/[Nb] = 0.946) were grown along the c axis using traditional Czochralski method in air. The doping concentrations of Yb^{3+} and Tm^{3+} ions were both 1 mol%. The doping concentrations of Hf^{4+} were 2 mol%, 4 mol%, and 6 mol%, respectively, which were referred to as Hf2, Hf4, and Hf6 for convenience. After precisely weighed, the raw materials with purity of 99.99% were thoroughly mixed for 24 h to grow high quality crystals. Subsequently, the raw materials were heated at 750 °C for 3 h to remove CO_2 and then sintered at 1150 °C for 4 h to form poly-crystals in single crystal furnace. The optimum conditions of the crystals growth were selected as follows: the temperature gradient of 30 °C/cm^{-1}, the rotating rate of 15–25 r/pm, and the pulling rate of 0.6–1.5 mm/h. After cooled down to room temperature with a speed of 50 °C/h, the crystals were polarized for 2 h at 1100 °C with the current density of 5 mA/cm^2. The grown sample Hf2 is shown in Fig. 1. Finally, the samples were cut into Y-cut plates with the dimensions of 10 mm×20 mm×2 mm ($x \times z \times y$) from the central part of the crystal and polished to optical grade.

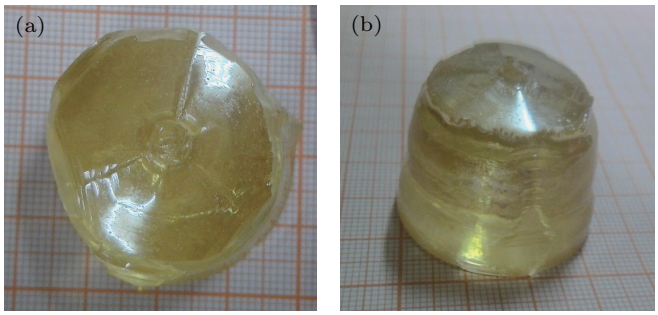


Fig. 1. (color online) The photo of sample Hf2: (a) top view, (b) front view.

2.2. Measurement

The lattice constant and crystal structure of the samples were characterized by a SHMADZU XRD-6000 diffractometer with Cu target. The angular range of the measurement is from 10° to 80° and the tube voltage/tube current is 40 kV/50 MA.

Since the O–H vibration is sensitive to the change of ionic environment, the position of O–H vibration absorption peak is used to analyze the defect structures of the doped crystals. The IR transmission spectra of the samples were measured at a resolution of 1 cm^{-1} by a Nicolet-710 FT-IR spectrometer with the effective range of 3400–3600 cm^{-1}.

The UV–VIS–NIR absorption spectra of the samples were measured by a Varian Cary 5000 spectrometer. The experiment conditions are as follows: room temperature, the range of 300–3000 nm, the measurement step distance of 1 nm, and the scanning rate of 600 nm/min.

The upconversion luminescence spectra of Hf:Yb:Tm:$LiNbO_3$ crystals were obtained under 980 nm excitation. The experimental system is shown in Fig. 2. A pump source which is obtained by 980 nm diode laser with excitation power of 600 mW excites the sample after focusing. Through the upconversion performance of the sample, the 980 nm laser converts into visible light. Furthermore, the upconversion luminescence spectra were recorded by Zolix-SBP300 grating spectrometer which is equipped with CR131 photomultiplier tube. The light signal is converted into an electrical signal and the intensity of the signal is amplified. Finally, the data is collected and the spectrum is displayed in the computer.

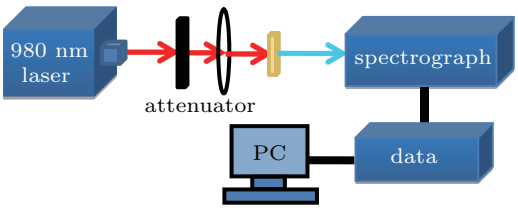


Fig. 2. (color online) The schematic diagram of upconversion luminescence experimental setup.

3. Results and discussion

XRD patterns of the Hf:Yb:Tm:$LiNbO_3$ crystals and the grown pure $LiNbO_3$ crystals are displayed in Figs. 3 and 4. It is obvious that there is no new diffraction peak compared with the pure $LiNbO_3$ structure. Hence, the diffraction patterns of the samples are indexed as hexagonal phase of $LiNbO_3$ crystal, which reflects that all grown crystals are single phase. According to the data of XRD, the lattice parameters were calculated by the least square method and listed in Table 1. The unit cell volumes were computed by the formula $V = a^2 c \cos 30°$. The lattice constants of the pure congruent $LiNbO_3$ crystal is shown in Table 1 for comparison.

It is clear that the unit cell volumes of the $LiNbO_3$ crystals change with the concentration of Hf^{4+} ions. Since the concentration of Li^+ is less than that of Nb^{5+} in pure congruent $LiNbO_3$ crystal, the anti-site Nb (Nb_{Li}^{4+}) and Li vacancy (V_{Li}^-) exist. As is known to us, three factors affect the unit cell volume: the concentration of V_{Li}^-, the polarization ability and ionic radius of the doping ions. When doping 2 mol% Hf^{4+}, 1 mol% Yb^{3+}, and 1 mol% Tm^{3+} ions, the unit cell volumes of $LiNbO_3$ crystals decrease. The reasons are as follows. Hf^{4+}, Yb^{3+}, and Tm^{3+} ions substitute Nb_{Li}^{4+} and V_{Li}^-

in the form of Hf_{Li}^{3+}, Yb_{Li}^{2+}, and Tm_{Li}^{2+}. Based on charge balance, Nb_{Li}^{4+}, Hf_{Li}^{3+}, Yb_{Li}^{2+}, and Tm_{Li}^{2+} defects need V_{Li}^{-} defects to form Nb_{Li}^{4+}–$4V_{Li}^{-}$, Hf_{Li}^{3+}–$3V_{Li}^{-}$, Yb_{Li}^{2+}–$2V_{Li}^{-}$, and Tm_{Li}^{2+}–$2V_{Li}^{-}$ defects. The doping ions reduce the concentration of Nb_{Li}^{4+} and increase the concentration of Hf_{Li}^{3+}, Yb_{Li}^{2+}, and Tm_{Li}^{2+}, which leads to the decrease of V_{Li}^{-} concentration followed by the decrease of unit cell volume. Another reason is that the polarization ability of Hf_{Li}^{3+} is higher than Nb^{5+} and V_{Li}^{-}. When the doping concentration of Hf^{4+} increases up to 4 mol%, Hf^{4+} ions replace the normal Li and Nb sites to constitute its own charge balance in the form of Hf_{Li}^{3+}–$3Hf_{Nb}^{-}$. Theoretically, the unit cell volume of $LiNbO_3$ crystal should also decrease. However, the unit cell volume increases gradually in the experiment. The reason may be that ionic radius becomes the main factor affecting the unit cell volume with the doping concentration of Hf^{4+} increased and the ionic radius of Hf^{4+} (0.81 Å[23]) ions is larger than that of Li (0.69 Å[24]) and Nb (0.68 Å[24]) ions.

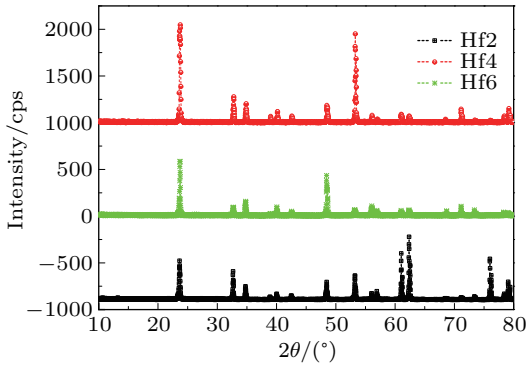


Fig. 3. (color online) XRD patterns of Hf:Yb:Tm:$LiNbO_3$ crystals.

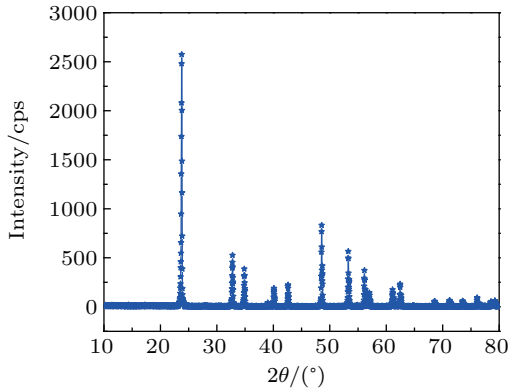


Fig. 4. (color online) XRD pattern of the pure congruent $LiNbO_3$ crystal.

Table 1. Lattice constants of Hf:Yb:Tm:$LiNbO_3$ crystals.

Sample	$a=b$/nm	Δa/nm	c/nm	Δc/nm	V/nm^3
$LiNbO_3$	0.5146	0	1.3852	0	0.31767
Hf2	0.5148	0.0002	1.3821	–0.0031	0.31721
Hf4	0.5155	0.0009	1.3834	–0.0018	0.31837
Hf6	0.5157	0.0011	1.3966	0.0114	0.32166

IR transmission spectra of Hf:Yb:Tm:$LiNbO_3$ crystals with various Hf^{4+} concentrations are shown in Fig. 5, in which the position of OH^- absorption peak shifts to the lager wavenumber with the increase of Hf^{4+} concentration. The OH^- absorption peak of sample Hf2 is located at 3484 cm^{-1}. While the OH^- absorption peaks of samples Hf4 and Hf6 are shifted to 3495 cm^{-1} and 3498 cm^{-1}, respectively. It is known that there are many intrinsic defects including anti-site Nb (Nb_{Li}^{4+}) and Li vacancy (V_{Li}^{-}) in congruent $LiNbO_3$ crystals and the OH^- absorption peak of congruent $LiNbO_3$ crystals is located at 3482 cm^{-1} owing to the OH^- stretching vibration of complex defect ($3V_{Li}^{-}$–Nb_{Li}^{4+}–OH^-).[25] Based on a large number of reports, the OH^- absorption peak of doped $LiNbO_3$ crystals will obvious shifts from about 3482 cm^{-1} of pure congruent $LiNbO_3$ crystals to lager wavenumber when the doping concentration exceed its thresholds.[25–27] The OH^- absorption peak at 3495 cm^{-1} indicates that the 4 mol% Hf^{4+} doping in Yb:Tm:$LiNbO_3$ crystal is up to the threshold concentration. This is similar to the previously reported threshold concentration in Hf:$LiNbO_3$ crystals.[26] In sample Hf2, the Hf^{4+}, Yb^{3+}, and Tm^{3+} ions enter into $LiNbO_3$ crystal by replacing Nb_{Li}^{4+} defects to form Hf_{Li}^{3+}, Yb_{Li}^{2+}, and Tm_{Li}^{2+} defects, which repel H^+ ions. As a result, the OH^- absorption peak of sample Hf2 still reflects the OH^- vibration around V_{Li}^{-} defects and is located at 3484 cm^{-1}. The slight shift is caused by the reducing of Nb_{Li}^{4+} and V_{Li}^{-} defects. When the doping level of Hf^{4+} exceeds its threshold in samples Hf4 and Hf6, Nb_{Li}^{4+} defects are replaced completely and partial Hf^{4+} ions begin enter the normal Li and Nb sites in the form of Hf_{Li}^{3+} and Hf_{Nb}^{-} defects. Since Hf_{Nb}^{-} defects have a stronger force to attract H^+ than V_{Li}^{-}, H^+ ions aggregate around Hf_{Nb}^{-} to form Hf_{Nb}^{-}–OH^- defects. Meanwhile more energy is required for OH^- stretching vibration. So the absorption peak that reflects the OH vibration around Hf_{Nb}^{-} shows blue shift.

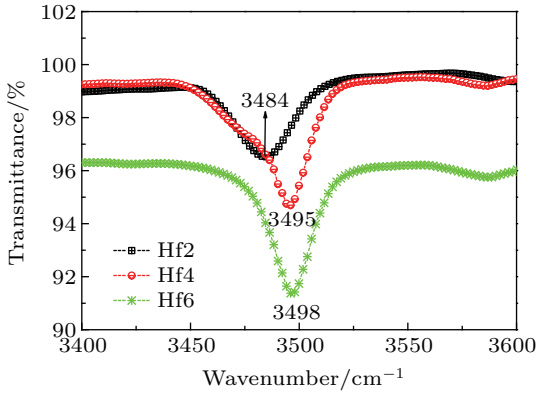


Fig. 5. (color online) IR transmission spectra of Hf:Yb:Tm:$LiNbO_3$ crystals.

The UV–VIS–NIR absorption spectra of Hf:Yb:Tm:$LiNbO_3$ crystals are shown in Fig. 6. Besides the absorption band centered at 980 nm caused by $^2F_{7/2} \rightarrow {}^2F_{5/2}$ transition of Yb^{3+} ions, the other absorption bands owe to the electronic transition of Tm^{3+} ions. The absorption bands centered at 703 nm, 795 nm, and 1215 nm are attributed to the transitions from

the ground state $^3H_6$ to the excited states $^3F_{2,3}$, $^3H_4$, and $^3H_5$. And the absorption bands centered at 1666 nm and 1757 nm both correspond to the transition from $^3H_6$ to $^3F_4$ due to the stark sublevel absorption caused by the crystal-field splitting in Hf:Yb:Tm:$LiNbO_3$ crystals. In addition, the absorption band centered at 2352 nm is attributed to the $^3H_5 \rightarrow ^3H_4$ transition of Tm^{3+} ions. Among these absorption bands, 980 nm which is well adapted for emission wavelength of commercial diode laser can be selected as the pump wavelength. By comparison of the absorption spectra, the following characteristics are identified. Firstly, the absorption spectra of samples Hf2, Hf4, and Hf6 are similar in the shape and band position, except disappearance of absorption band centered at 2352 nm in sample Hf6. Since the Tm^{3+} doped crystal has a potential application for 2–2.5 μm laser, the high doping Hf^{4+} ions will eliminate the absorption at this wavelength and be benefit for the application. Secondly, the intensities of the absorption bands first increase and then decrease with the increase of Hf^{4+} ions concentration.

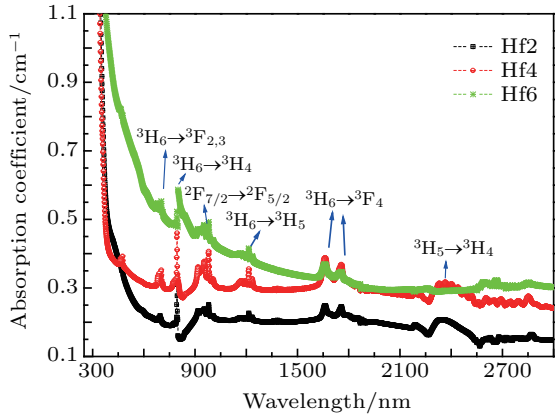


Fig. 6. (color online) The UV–VIS–NIR absorption spectra of the Hf:Yb:Tm:$LiNbO_3$ crystals.

Upconversion luminescence spectra of Hf:Yb:Tm:$LiNbO_3$ crystals in the visible wavelength range excited by 980 nm laser diode are shown in Fig. 7. The strongest intensity peak is centered at 475 nm in the blue wavelength range. This peak is attributed to the $^1G_4 \rightarrow ^3H_6$ transition of Tm^{3+} ions. Another peak is centered at 651 nm in the red wavelength range and attributed to the $^1G_4 \rightarrow ^3F_4$ transition. Compared with sample Hf2, the intensity of blue and red emissions increases obviously in samples Hf4 and Hf6. Especially, in sample Hf6, the blue emission is about 4.7 times and the red emission is about 1.9 times more than that in sample Hf2. It is obvious that the increase of Hf^{4+} doping concentration is beneficial for upconversion luminescence of Hf:Yb:Tm:$LiNbO_3$ crystals.

As is well known, the intensity of upconversion luminescence is closely related to the local environment, the doping concentration, and the distribution of active ions in a host material.[20] In consideration of the fixed Tm^{3+} and Yb^{3+} ions concentration, the change of the intensity of upconversion luminescence is caused by the local environment of Tm^{3+} and Yb^{3+} ions adjusted by Hf^{4+} ions. One reason for the enhancement is the minimization of structural defects in crystals. The atomic radius difference of Li (1.54 Å) and Nb (1.48 Å) is more remarkable than Hf (1.59 Å). Hence, doping Hf^{4+} ions that reduce V_{Li}^{-} defects and replace Nb_{Li}^{4+} defects to form Hf_{Li}^{3+} will minimize the structural defects of the crystal. Another reason is explained as follows. As we have known, three and two photons are involved in the blue and red upconversion emissions, respectively. The energy transfer mechanism of upconversion process in Hf:Yb:Tm:$LiNbO_3$ crystals is shown in Fig. 8. In the upconversion process, Yb^{3+} ions are excited from the ground state $^2F_{7/2}$ to the $^2F_{5/2}$ state by absorbing 980 nm NIR photon via ground state absorption (GSA). Then the energy transfers from Yb^{3+} to Tm^{3+} ions followed by populating $^3H_5$, $^3F_2$, and $^1G_4$ intermediate states of Tm^{3+} ions. The $^3H_5 \rightarrow ^3F_4$ and $^3F_2 \rightarrow ^3H_4$ transitions of Tm^{3+} ions are achieved by nonradiative relaxation. Finally, blue and red upconversion emissions are obtained though the $^1G_4 \rightarrow ^3H_6$ and $^1G_4 \rightarrow ^3F_4$ transitions respectively in radiative relaxation progress. However, the existence of cross relaxation (CR) processes ($^3H_4 + ^3H_6 \rightarrow ^3F_4 + ^3F_4$) will suppress the population of $^3H_4$.[28] Because the excited state absorption (ESA) which is an inherent result of a given pump choice is hard to change and CR processes can be suppressed by decrease of Tm^{3+} cluster

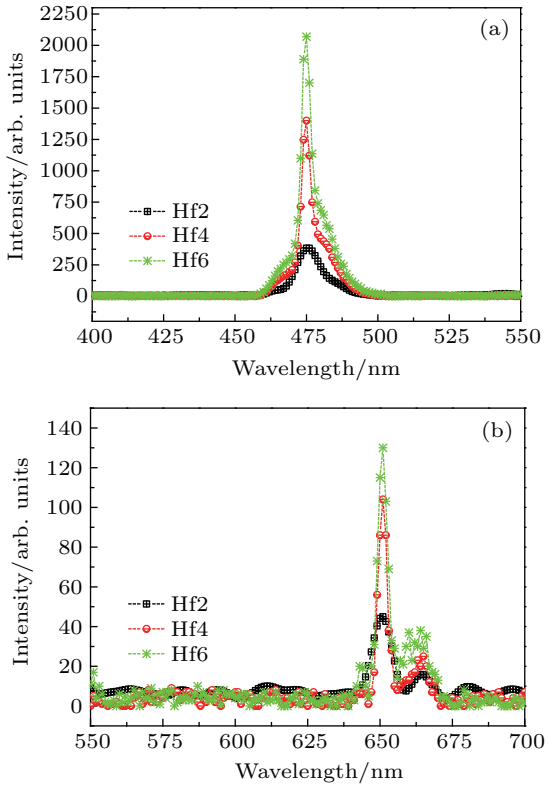


Fig. 7. (color online) Room-temperature upconversion luminescence spectra of Hf:Yb:Tm:$LiNbO_3$ crystals: (a) 400–550 nm, (b) 550–700 nm.

sites.[29–31] The enhancement of upconversion emission indicates the suppression of CR processes and reduction of Tm^{3+} cluster sites, which is caused by high doping Hf^{4+} ions. In conclusion, Hf^{4+} ions can improve the luminescence environment and enhance the intensity of blue and red emissions in Hf:Yb:Tm:$LiNbO_3$ crystals.

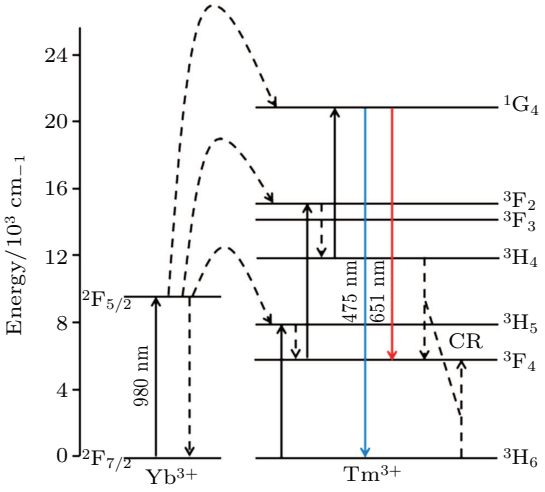


Fig. 8. (color online) The energy levels of Yb^{3+} and Tm^{3+} ions as well as the upconversion luminescence mechanism of Hf:Yb:Tm:$LiNbO_3$ crystals.

4. Conclusion

In this work, Hf:Yb:Tm:$LiNbO_3$ crystals with variable Hf^{4+} concentrations have been successfully grown by the Czochralski method. The IR transmission spectrum indicates that Nb_{Li}^{4+} defects are replaced completely and Hf^{4+} ions begin enter the normal Li and Nb sites when the Hf^{4+} doping concentration is up to 4 mol%. The UV–VIS–NIR absorption spectra first increase and then decrease with the increase of Hf^{4+} ions concentration and display strong absorption peaks at 980 nm. Under excitation at this wavelength, the blue (475 nm) and red (651 nm) upconversion luminescences are achieved though the $^1G_4 \rightarrow {}^3H_6$ and $^1G_4 \rightarrow {}^3F_4$ transitions of the Tm ions. The blue emissions intensity of 6 mol% Hf^{4+} tridoped Yb:Tm:$LiNbO_3$ crystal is about 4.7 times larger than that of 2 mol% Hf^{4+} tridoped Yb:Tm:$LiNbO_3$ crystal and the red emission intensity enhances by 1.9 times. The upconversion luminescence spectra remarkably increase with the increase of Hf^{4+} doping concentration. The generation and enhancement of the blue and red upconversion luminescence in Hf:Yb:Tm:$LiNbO_3$ crystals are interesting for solid-state lasers and color display.

References

[1] Mokoena T P, Linganiso E C, Kumar V, Swart H C, Cho S H and Ntwaeaborwa O M 2017 *J. Colloid Interface Sci.* **496** 87

[2] Dai L, Liu C R, Tan C, Yan Z H and Xu Y H 2017 *Chin. Phys. B* **26** 044207

[3] Fischer S, Goldschmidt J C, Loper P, Bauer G H, Bruggemann R, Kramer K, Biner D, Hermle M and Glunz S W 2010 *J. Appl. Phys.* **108** 044912

[4] Lu H C, Yi G S, Zhao S Y, Chen D P, Guo L H and Cheng J 2004 *J. Mater. Chem.* **14** 1336

[5] Mialon G, Türkcan S, Dantelle G, Collins D P, Hadjipanayi M, Taylor R A, Gacoin, T, Alexandrou A and Boilott J P 2010 *J. Phys. Chem. C* **114** 22449

[6] Joubert M F 1999 *Opt. Mater.* **11** 181

[7] Tumuluri A, Bharati M S S, Rao S V and Raju K C J 2017 *Mater. Res. Bull.* **94** 342

[8] Wu L, Ling F R, Zuo Z G, Liu J S and Yao J Q 2012 *Chin. Phys. B* **21** 017802

[9] Zhang D L, Qiu C X, Wong W H and Pun E Y B 2014 *Mater. Res. Bull.* **60** 771

[10] Wang Z J, Li X Z, Wei Q and Long X F 2008 *Mater. Res. Innov.* **12** 174

[11] Mahalingam V, Naccache R, Vetrone F and Capobianco J A 2012 *Opt. Express* **20** 111

[12] Xing L L, Yang W Q, Lin J C, Huang M and Xue Y Q 2017 *Sci. Rep.* **7** 14725

[13] Xing L L, Xu Y L, Wang R, Xu W and Zhang Z G 2014 *Opt. Lett.* **39** 454

[14] Xu Z P, Bi W H, Jiao B L, Ben Y Z, Lu Q Z and Tang H H 2010 *Cryst. Res. Technol.* **45** 85

[15] Sidorov N V, Palatnikov M N, Yanichev A A, Titov R A and Makarova O V 2017 *Tech. Phys.* **62** 417

[16] Zhen X H, Li Q, Li H T, Xu Y H and Zhao L C 2005 *Cryst. Res. Technol.* **40** 649

[17] Zhang T, Wang B, Fang S Q, Ma D C, Zhao Y Q and Xu Y H 2004 *Mater. Lett.* **58** 3074

[18] Sun X D, Shi H X, Luo S H, Meng Q X and Jiang Y Y 2010 *Chin. Phys. B* **19** 094209

[19] Dai L, Jiao S S, Xu C, Li D Y, Lin J Q and Chen C T 2014 *Mater. Res. Bull.* **53** 132

[20] Qian Y N, Zhang Z Y, Tang X Z, Ivanov M, Zhang H Y and Wu Q B 2017 *Opt. Mater.* **70** 116

[21] Shur J W, Choi K H and Yoon D H 2011 *J. Cryst. Growth* **318** 653

[22] Sun L, Yang C H, Li A H, Xu Y H and Zhao L C 2009 *J. Appl. Phys.* **105** 043512

[23] Lorenzo A, Jaffrezic H and Roux B 1995 *Appl. Phys. Lett.* **67** 3735

[24] Mignotte C 2001 *Appl. Surf. Sci.* **185** 11

[25] Xu Z P, Xu S W, Xu Y H and Wang R 2005 *Mod. Phys. Lett. B* **19** 1277

[26] Li S Q, Liu S G, Kong Y F, Deng D L, Gao G Y, Li Y B, Gao H C, Zhang L, Hang Z H, Chen S L and Xu J J 2006 *J. Phys.: Condens. Matter* **18** 3527

[27] Zhang T, Wang X, Geng T, Tong C G and Kang C 2015 *J. Alloys Compd.* **629** 255

[28] Jackson S D and Mossman S 2003 *Appl. Opt.* **42** 2702

[29] Qian Y N, Wang R, Xing L L, Xu Y L, Yang C H and Liu X R 2011 *Cryst. Res. Technol.* **46** 1137

[30] Renard S, Camy P, Doualan A B J L and Moncorge R 2008 *J. Alloys Compd.* **451** 71

[31] Jackson S D 2004 *Opt. Commun.* **230** 197